1 June 2001

ELSEVIER

Chemical Physics Letters 340 (2001) 282–288

CHEMICAL PHYSICS LETTERS

www.elsevier.nl/locate/cplett

Reaction mechanism for the oxidation of free silver dimers

Liana D. Socaciu, Jan Hagen, Ueli Heiz [1], Thorsten M. Bernhardt *, Thomas Leisner [2], Ludger Wöste

Institut für Experimentalphysik, Freie Universität Berlin, Arnimallee 14, D-14195 Berlin, Germany

Received 26 October 2000; in final form 17 April 2001

Abstract

The kinetics of the interaction of Ag_2^+ with O_2 is studied in the gas phase under multi-collision conditions at various temperatures. A new experimental scheme is employed, which consists of an octopole ion trap of variable temperature inserted into a tandem quadrupole mass spectrometer. From the time evolution of the reactant and product molecule concentrations at different temperatures the corresponding reaction mechanism is extracted. Surprisingly, the product Ag_2O^+ is detected, which is formed after molecular adsorption and dissociation of O_2. We can clearly identify $Ag_2O_2^+$ as an intermediate in this reaction. In addition, absolute rate coefficients and activation energies for the molecular adsorption of O_2 onto Ag_2^+ are presented.

1. Introduction

Recent experiments on nano-assembled model catalysts consisting of size-selected clusters on oxide surfaces reveal striking changes in the size-dependent evolution of the efficiency and selectivity of catalytic processes like the oxidation of CO on small Au_n, Pt_n, Pd_n, and Rh_n clusters or the polymerization of acetylene on small Pd_n clusters [1,2]. These studies show that charging small clusters via charge transfer from the substrate is essential for turning clusters into active catalysts [1]. Ion chemistry of small metal clusters is thus relevant for real catalysis. Furthermore, the combination of experiments on free and supported clusters as well as ab initio calculations will give an understanding of catalytic processes on the molecular level.

In the last two decades adsorption and reactions on free charged and neutral metal clusters were extensively studied, and concepts for cluster reactivities were extracted from the large amount of experimental data. Several experimental schemes were introduced for studying chemical properties of free clusters. After the clusters are produced by various cluster sources the actual reactions are performed in fast flow reactors [3–10], quadrupole [11,12] and octopole ion guides [13,14], Penning traps [15] or Fourier transform ion cyclotron resonance mass spectrometry (FTICR-MS) [16–20]. In all experimental schemes the reaction products are then analyzed by mass spectrometry. Cluster reactivities are extracted from measurements of cluster size distributions. To prevent possible contributions from fragmen-

* Corresponding author. Fax: +49-30-838-55567.

E-mail address: tbernhar@physik.fu-berlin.de. (T.M. Bernhardt).

[1] Present address: Abteilung für Oberflächenchemie und Katalyse, Universität Ulm, D-89069 Ulm, Germany.

[2] Present address: Institut für Physik, Technische Universität Ilmenau, D-98684 Ilmenau, Germany.

0009-2614/01/$ - see front matter
PII: S0009-2614(01)00447-X

tation of larger cluster sizes the experimental schemes were refined by mass-selecting clusters prior to reaction [12,14]. All these studies lead to the characterization of stable cluster complexes, e.g., products of the chemical reaction [3,4,9,12,17,21], the extraction of reaction probabilities [6,7,10] or even to the measurement of absolute rate coefficients at a given temperature [8,15,19,20]. In few examples a full thermal catalytic cycle was studied [14,16]. To our knowledge, however, none of these studies revealed the temperature-dependent kinetics of a metal cluster reaction, which is needed for obtaining reaction mechanisms of a chemical process at thermodynamically controlled conditions and for extracting kinetic data like absolute rate coefficients and activation energies.

In this work, we present an experimental scheme, where the clusters are size-selected and subsequently stored in an octopole ion trap of variable temperature. The thermalized clusters, in the present example Ag_2^+, react with reactants like O_2 at well-defined thermodynamic conditions. The charged products of this oxidation reaction are then analyzed by mass spectrometry as function of the reaction time and temperature. The measured kinetic data are modeled with different reaction mechanisms, and absolute rate coefficients and activation energies are determined for the best fit.

Interestingly, neutral Ag_2 is unreactive against O_2 in a fast flow reactor at ambient temperature [5]. Hydroxide formation has been observed in the reactive nucleation of neutral Ag_n with oxygen in the presence of water traces [22]. Also in a flow tube reactor, negatively charged silver clusters react with oxygen under exclusive formation of $Ag_nO_2^-$ products [23]. In this Letter, we report the first investigation of the reaction of positively charged silver clusters with oxygen. Our new experimental approach reveals that already the dimer cluster of silver exhibits a rich reaction kinetics. We observe intermediate molecularly adsorbed O_2 and temperature-dependent dissociation reaction on the cluster.

2. Experimental

The main experimental setup is described in detail elsewhere [24] and only brief details are given here (Fig. 1). The cluster cations are produced by a sputter source and are extracted into a helium-filled quadrupole (Q_0), where they are cooled down to room temperature and collimated to the axis of the ion optics. A second quadrupole (Q_1) selects a single cluster size. The cluster ions are then transferred with a quadrupole ion guide (Q_2) into a homebuild octopole ion trap, which can be continuously cooled from $T_T = 350$ to 20 K. The

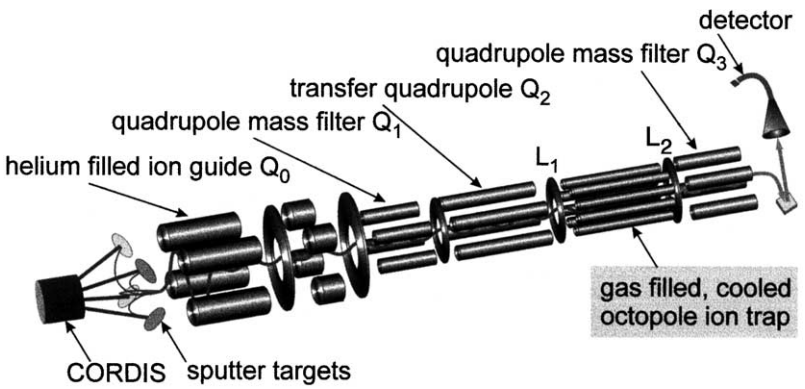

Fig. 1. Experimental setup for the investigation of reaction kinetics of metal clusters. The cluster ions are sputtered from solid targets with a cold reflex discharge ion source (CORDIS), mass-selected (Q_1), and guided at low energies (Q_0 and Q_2) into the temperature controllable octopole ion trap. By means of appropriate switching of the lenses L_1 and L_2 the reaction products are extracted and subsequently mass-analyzed by another quadrupole mass filter (Q_3).

potentials on the entrance and exit lenses, L_1 and L_2, can computationally be switched in order to fill the trap, store the ions in the trap, and finally extract product ions for mass analysis. Through collisions with a buffer gas (helium or argon) in the trap, the clusters are thermalized. Different reactants, e.g., O_2, can be added to the ion trap, and the corresponding partial pressures p_R are measured with a baratron (MKS, Typ 627B). After reaction time t_R, the charged products are extracted from the trap and are analyzed by a quadrupole mass spectrometer (Q_3) as function of t_R, p_R, and T_T. The ion pulses are amplified by a channeltron/conversion dynode detector and digitalized and integrated by a LeCroy 9400A 175 MHz oscilloscope.

Space charge effects limit the maximal cluster density in the octopole ion trap to a fixed amount of 1.1×10^4 mm^{-3}. This value represents the initial concentration of the reactant Ag_2^+ for all the results presented in this work. In addition, for optimal performance the ion trap is filled with a buffer gas density of about 2×10^{12} mm^{-3}. For the reaction studies the reactants are mixed to the buffer gas, and a ratio between rare gas and O_2 of four is used for all experiments. From these numbers the following conclusions are drawn: (1) Statistical theory of cluster cooling in rare gases shows that thermally excited clusters are thermalized already within 2000 collisions with the buffer gas [25]. The collision frequency in our experiment is about 3×10^5 s^{-1} and therefore cluster temperatures are in thermal equilibrium with the ion trap already after a few milliseconds [26]; (2) The density of the reactant is orders of magnitudes larger than the cluster density; in addition, there is a steady flow of O_2 during reaction. Thus, the oxygen concentration is taken constant for modeling the kinetics; (3) Reaction products are only reacting further with O_2 and not with each other (low density, Coulomb repulsion between charged products). In addition, collision-induced fragmentation is unambiguously excluded under our experimental conditions as no fragments are detected by using different buffer gases (He, Ar). Also the RF-frequency of the octopole ion trap is chosen such that field-induced fragmentation of even the most weakly bound reactant Ag_2^+ is minimized (<5%). Thus, the RF-induced velocity component can be considered not to exceed significantly conditions given by the surrounding gas temperature.

3. Results

Surprisingly, no products $Ag_2O_n^+$ with $n > 4$ are observed for temperatures between 50 and 300 K under our experimental conditions. In addition, the distribution of the reaction products reveals a strong temperature dependence. Fig. 2 shows product mass spectra obtained at three different reaction temperatures (50, 95, and 130 K) under otherwise comparable experimental conditions. At 50 K the exclusive oxidation products are $Ag_2O_2^+$

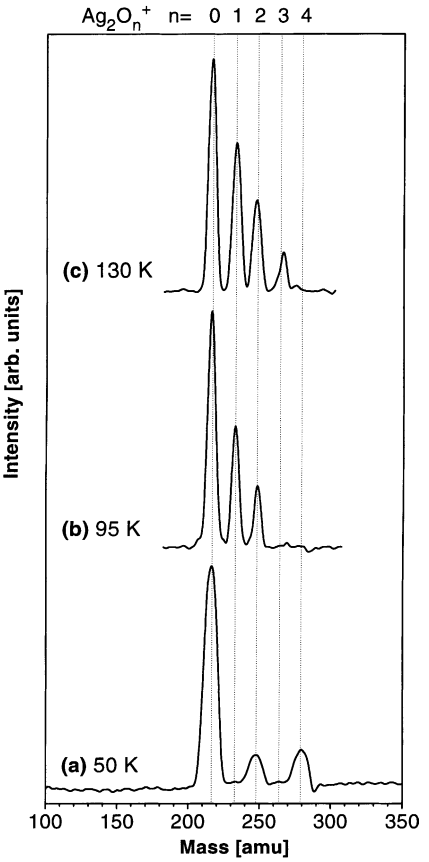

Fig. 2. Product ion mass spectra of the reaction of Ag_2^+ with O_2 at three different temperatures T_T ((a) 50 K, (b) 95 K, (c) 130 K) under otherwise comparable conditions.

and $Ag_2O_4^+$ at all reaction times up to 10 s, which points toward molecular adsorption of a maximum of two O_2 molecules. The mass distribution of the products changes drastically at higher temperatures. At 95 K the new product Ag_2O^+ appears and no $Ag_2O_4^+$ is observed anymore. At even higher temperatures (130 K) $Ag_2O_3^+$ is detected as the largest product. These results indicate a strongly temperature-dependent reaction mechanism. In order to extract possible reaction schemes, the reactant and product concentrations are measured as function of the reaction time. The results for three temperatures (95, 110, and 130 K) are depicted in Fig. 3. The evolution of the Ag_2^+ concentration with reaction time shows a multi-exponential decay at all temperatures. The reaction time for a 50% decay of the initial concentration clearly decreases with increasing temperature, which is indicative for activated processes. $Ag_2O_2^+$ is identified as an intermediate product with maximum concentration at very short reaction times and increasing amplitude for higher reaction temperatures. The final product at 95 and 110 K is Ag_2O^+, whereas at 130 K the new product $Ag_2O_3^+$ appears with a delay of about 2 s.

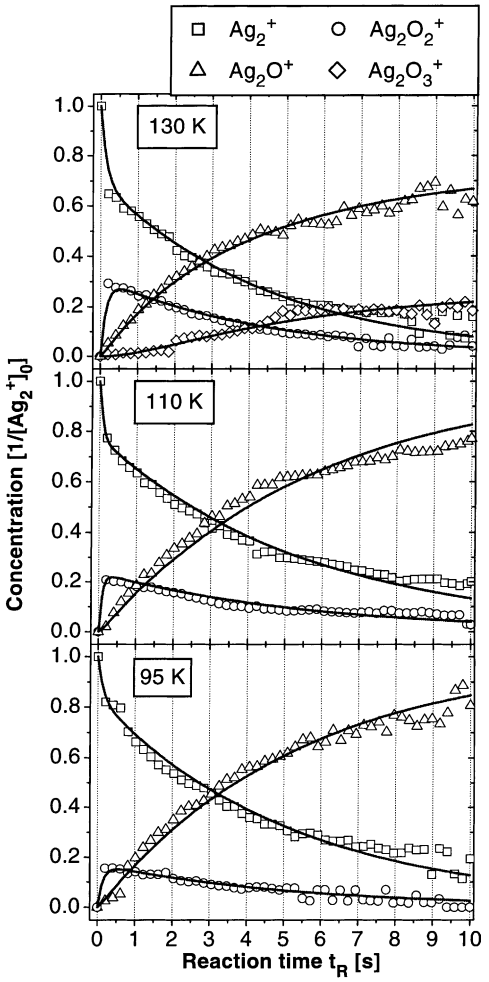

Fig. 3. Product ion concentrations of the reaction $Ag_2^+ + O_2$ as a function of the reaction time t_R for $T_T = 95$, 110, and 130 K. The open symbols represent the experimental data, normalized on the initial Ag_2^+ concentration and on the total ion concentration in the trap, which decreases over 10 s by only about 5%. The solid lines are obtained by fitting the integrated rate equations of the proposed reaction mechanism to the experimental data.

4. Discussion

These experimental findings suggest the following reaction mechanism:

$$Ag_2^+ + O_2 \rightleftarrows Ag_2O_2^+ \quad k_1, k_2\ [E_{a,1}, E_{a,2}]$$
$$Ag_2O_2^+ \rightarrow Ag_2O^+ + O \quad k_3\ [E_{a,3}]$$
$$Ag_2O^+ + O_2 \rightleftarrows Ag_2O_3^+ \quad k_4, k_5\ [E_{a,4}, E_{a,5}]$$

k_1–k_5 are the rate coefficients for the different reaction steps and $E_{a,1}$–$E_{a,5}$ are the corresponding activation energies. $Ag_2O_2^+$ is unambiguously identified as an intermediate (cf. Fig. 3) and is formed in a first elementary step by molecular adsorption of O_2 onto Ag_2^+. Molecular adsorption of up to two O_2 molecules has been observed at lower temperatures (50 K, Fig. 2a). $Ag_2O_4^+$ is however not a stable product at higher temperatures. In a second elementary step Ag_2O^+ is formed by dissociation of the adsorbed O_2 molecule. The dissociation of O_2 is not observed at 50 K, as the corresponding activation energy is thermally not reached. Increasing the temperature to 130 K results in a further product, $Ag_2O_3^+$. This third elementary step is observed at delayed reaction times and consists of molecular adsorption of O_2 to Ag_2O^+.

The validity of this mechanism is tested by fitting the corresponding integrated rate equations

simultaneously to the experimental kinetic data of Ag_2^+ and all observed reaction products. The rate equations of the equilibrium and consecutive reaction steps have been integrated numerically by using the fourth-order Runge–Kutta algorithm. The employed fitting procedure consists of an iterative non-linear least-square method [27]. As already discussed in Section 2, the oxygen concentration in the octopole trap is constant and therefore all reaction steps are taken as pseudo first-order in the simulations. As shown in Fig. 3, the fitted kinetics of the reaction mechanism describe well the experimental data. In order to further establish this mechanism, other reaction mechanisms were also fitted to the experimental data. We particularly note that purely consecutive reaction steps do not fit the data. This supports the necessity of incorporating equilibrium steps for the reaction of O_2 with Ag_2^+ and Ag_2O^+ and confirms the molecular adsorption of O_2 on these two ions.

The observed influence of different buffer gases (Ar, He) on the rate constants indicates that the equilibrium steps should in detail be described by the Lindemann mechanism for association reactions [28], which assumes that a three body collision is necessary to stabilize the reaction product. Considering the collision frequency under the present experimental conditions (10^5 s^{-1}) and an estimated lifetime of the activated complex after the bimolecular reaction on the order of less than 10 ns [23], we assume that the measured bimolecular rate coefficients are pressure-dependent (low pressure limit of Lindemann mechanism [3]). This however has no influence on the corresponding activation energies. The absolute bimolecular rate coefficients (Table 1) are obtained by fitting the analytically integrated rate equation to the time evolution of the Ag_2^+ concentration and by measuring the partial pressure of oxygen in the trap (0.003 mbar in all experiments).

Table 1
Bimolecular rate coefficients for the reaction of Ag_2^+ with O_2 at different temperatures at 0.015 mbar total pressure

T (K)	k_1 (10^{-15} cm^3 s^{-1})	k_2 (10^{-15} cm^3 s^{-1})
130	30 ± 18	53 ± 36
110	7.4 ± 1.0	13.4 ± 2.7
95	2.5 ± 0.3	2.9 ± 0.7

This example shows that by measuring the temperature-dependent kinetics of a cluster reaction at thermodynamically controlled conditions a complex reaction mechanism can be extracted. In addition, it is possible to determine the absolute rate coefficients and activation energies of the corresponding elementary reaction steps. An estimation for the activation energies of the first equilibrium reaction $E_{a,1}$ and $E_{a,2}$ is obtained from the Arrhenius plots shown in Fig. 4.

The obtained results allow the construction of the potential energy surface along the reaction coordinate for the established reaction mechanism of the oxidation of silver dimer cations. Fig. 5 shows the proposed reaction path starting with the total binding energy of free Ag_2^+ (1.570 eV [29]) and O_2 (5.080 eV [30]), which is defined to be the origin (0 eV) of the energy scale. The first energy barrier for the formation of the product $Ag_2O_2^+$, according to the Lindemann mechanism discussed above, is given by $E_{a,1}$ (68 meV). If the interaction of O_2 with Ag_2^+ is modeled with a simple ion/induced dipole interaction potential [28], an activation barrier of about 50 meV is obtained, which is in good agreement with the experimental value. The measured activation energy for the back reaction $E_{a,2}$, i.e., the collision-induced decomposition of $Ag_2O_2^+$ amounts to 91 meV. The energy of

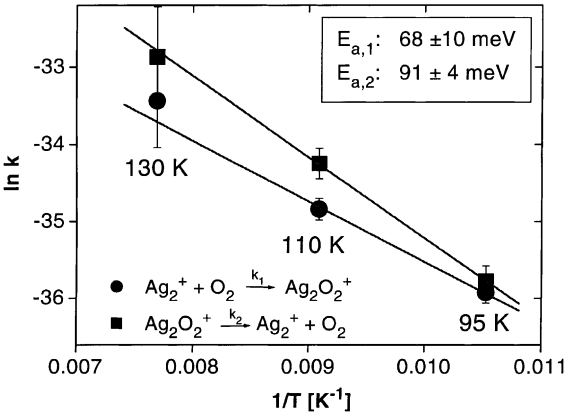

Fig. 4. Arrhenius plot for the first equilibrium reaction: $Ag_2^+ + O_2 \leftrightarrows Ag_2O_2^+$. The activation energies $E_{a,1}$ and $E_{a,2}$ are obtained from the linear regression fits.

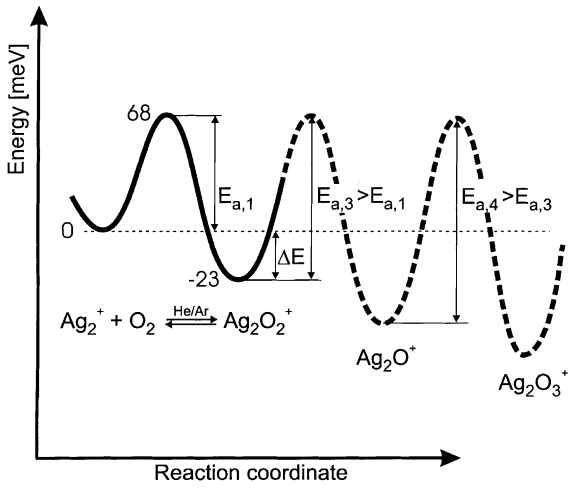

Fig. 5. Schematic potential energy surface for the reaction $Ag_2^+ + O_2$ along the reaction coordinate as discussed in the text.

the product $Ag_2O_2^+$ relative to the educts is given by the difference of the two activation energies ($\Delta E = 23$ meV). For comparison it is interesting to consider O_2 adsorption on single crystal surfaces. On the highly reactive Ag(1 1 0) surface oxygen adsorbs in four different states, depending on the surface temperature: below 40 K the O_2 is bound in a physisorbed state; in the range between 40 and 170 K it is molecularly chemisorbed, and at higher temperatures the molecules dissociate on the surface and chemisorb atomically [31].

The absence of the product ion Ag_2O^+ at the lowest temperature of 50 K indicates that the activation energy $E_{a,3}$ for the formation of this product through breakage of the O–O bond is higher than $E_{a,1}$ and $E_{a,2}$. For comparison, the activation energy for O_2 dissociation on surfaces amounts to 350 meV for the Ag(1 1 0) surface [31] and the heat of dissociative adsorption of O_2 on a polycrystalline silver surface was measured to be −640 meV [32]. From the presented data it is however not yet possible to obtain reliable absolute values for $E_{a,3}$. An extended investigation over a broad temperature range and for different cluster sizes is in progress [33]. At 130 K $Ag_2O_3^+$ is an additional product. This ion is formed by molecular adsorption of another oxygen molecule onto Ag_2O^+. This is inferred by the necessity to incorporate an equilibrium step in the reaction mechanism at this point, in order to properly fit the experimental data (Fig. 3). The observation, however, that the $Ag_2O_3^+$ product only appears at elevated temperatures of more than 130 K points toward an even larger activation barrier for this last step ($E_{a,4} > E_{a,3} > E_{a,1}$). The apparent difference in the activation energies for the molecular adsorption of O_2 on Ag_2^+ and on Ag_2O^+ can be understood, if we consider that any Ag_2O^+-structure must be permanently polarized, e.g., the dipole moment of $(Ag–Ag–O)^+$. Therefore, the interaction with O_2 has to be described in this case by a ion-dipole/induced dipole potential which leads to a higher reaction barrier compared to the ion/induced dipole potential discussed above [28].

5. Conclusion

This study reveals the detailed mechanism of a metal cluster reaction as well as absolute rate coefficients and activation energies, which aim to deduce the general shape of the potential energy surface along the reaction path. The results are based on temperature-dependent measurements of the reaction kinetics under multi-collision conditions in a new experimental setup. The appearance of the different product ions in the mass spectra as a function of the reaction temperature together with the concentration evolution as a function of reaction time leads to the proposed reaction mechanism, which is verified by fitting the integrated rate equations to the kinetic data. From the multi-exponential decay of the initial Ag_2^+ concentration absolute rate coefficients and activation energies are estimated.

The presented new and versatile approach to the study of metal cluster reactions will be extended to the investigation of larger and differently charged cluster ions of silver. This is especially important for the investigation of the role of molecularly and atomically adsorbed oxygen in the catalytic epoxidation of ethylene [34]. We also plan to study catalytically relevant reactions with various adsorbates on other noble metal clusters.

Acknowledgements

The authors are pleased to acknowledge fruitful discussions with Vlasta Bonačić-Koutecký and Vincent Veyret. We also thank Hannu Häkkinen for helpful suggestions. Financial support by the Deutsche Forschungsgemeinschaft (SFB 450) is gratefully acknowledged. U.H. thanks the Alexander von Humboldt-Foundation for a fellowship.

References

[1] U. Heiz, W.-D. Schneider, J. Phys. D 33 (2000) R85.
[2] M. Haruta, Catalysis Today 36 (1997) 153.
[3] R.E. Leuchtner, A.C. Harms, A.W. Castleman Jr., J. Chem. Phys. 92 (1990) 6527.
[4] D.M. Cox, R.O. Brickman, K. Creegan, A. Kaldor, Mater. Res. Soc. Symp. Proc. 206 (1991) 43.
[5] L. Lian, P.A. Hackett, D.M. Rayner, J. Chem. Phys. 99 (1993) 2583.
[6] J. Mwakapumba, K.M. Ervin, Int. J. Mass Spectrom. Ion Proc. 161 (1997) 161.
[7] L. Holmgren, M. Andersson, A. Rosén, Chem. Phys. Lett. 296 (1998) 167.
[8] D.B. Pederson, J.M. Parnis, D.M. Rayner, J. Chem. Phys. 109 (1998) 551.
[9] B. Kaiser, T.M. Bernhardt, M. Kinne, K. Rademann, J. Chem. Phys. 110 (1999) 1437.
[10] Q. Wu, S. Yang, Int. J. Mass Spectrom. 184 (1999) 57.
[11] S. Vajda, S. Wolf, T. Leisner, U. Busolt, L. Wöste, J. Chem. Phys. 107 (1997) 3492.
[12] K.A. Zemski, R.C. Bell, A.W. Castleman Jr., Int. J. Mass Spectrom. 184 (1999) 119.
[13] M.J. Jarrold, J.E. Bower, J. Chem. Phys. 87 (1987) 5728.
[14] Y. Shi, K.M. Ervin, J. Chem. Phys. 108 (1998) 1757.
[15] G. Dietrich, K. Dasgupta, S. Kuznetsov, K. Lützenkirchen, L. Schweikhard, J. Ziegler, Int. J. Mass Spectrom. Ion Proc. 157–158 (1996) 319.
[16] P. Schnabel, K.G. Weil, M.P. Irion, Angew. Chem. 104 (1992) 633.
[17] P. Jackson, K.J. Fisher, G.E. Gadd, I.G. Dance, D.R. Smith, G.D. Willett, Int. J. Mass Spectrom. Ion Proc. 164 (1997) 45.
[18] C. Berg, M. Beyer, U. Achatz, S. Joos, G. Niedner-Schatteburg, V.E. Bondybey, Chem. Phys. 239 (1998) 379.
[19] A.B. Vakhtin, K. Sugawara, Chem. Phys. Lett. 299 (1999) 553.
[20] M.C. Oliveira, J. Marcalo, M.C. Vieira, M.A. Almoster Ferreira, Int. J. Mass Spectrom. Ion Proc. 185–187 (1999) 825.
[21] A. Nakajima, T. Hayase, F. Hayakawa, K. Kaya, Chem. Phys. Lett. 280 (1997) 381.
[22] C. Bréchignac, P. Cahuzac, J. Leygnier, I. Tignères, Chem. Phys. Lett. 303 (1999) 304.
[23] T.H. Lee, K.M. Ervin, J. Phys. Chem. 98 (1994) 10023.
[24] H. Hess, S. Kwiet, L. Socaciu, S. Wolf, T. Leisner, L. Wöste, Appl. Phys. B 71 (2000) 337.
[25] J. Westergren, H. Grönbeck, A. Rosén, J. Chem. Phys. 109 (1998) 9848.
[26] D. Gerlich, in: C.-Y. Ng, M. Baer (Eds.), State-Selected and State-to-State Ion-Molecule Reaction Dynamics, Part 1: Experiment, Wiley, New York, 1992.
[27] E. Schumacher, DETMECH – Chemical Reaction Kinetics Software, Chemistry Department, University of Bern, 1997.
[28] J.I. Steinfeld, J.S. Francisco, W.L. Hase, Chemical Kinetics and Dynamics, Prentice-Hall, Englewood Cliffs, NJ, 1999.
[29] V. Beutel, G.L. Bahle, M. Kuhn, W. Demtröder, Chem. Phys. Lett. 185 (1991) 313.
[30] G. Herzberg, Molecular Spectra and Molecular Structure. I. Spectra of Diatomic Molecules, Van Nostrand Reinhold, New York, 1950.
[31] F. Besenbacher, J.K. Nørskov, Prog. Surf. Sci. 44 (1993) 5.
[32] C.N.R. Rao, P.V. Kamath, S. Yashonath, Chem. Phys. Lett. 88 (1982) 13.
[33] J. Hagen, L.D. Socaciu, U. Heiz, T.M. Bernhardt, L. Wöste, to be published.
[34] B.C. Gates, Catalytic Chemistry, Wiley, New York, 1991.